

Bed topography and surges in ice streams

Christian Schoof

Department of Earth and Ocean Sciences, University of British Columbia, Vancouver, British Columbia, Canada

Received 9 October 2003; revised 3 February 2004; accepted 26 February 2004; published 31 March 2004.

[1] Extensive bed topography at the scale of the ice thickness occurs frequently in the form of drumlins. By analogy with hard-bed sliding, ice flow over this type of topography leads to the generation of drag on the ice, particularly when ice flow is rapid. A crucial difference with classical Nye-Kamb sliding is that the upper, free surface of the ice has a significant effect on the sliding process through the formation of a standing wave. Using a theoretical model, we demonstrate that the presence of this wave introduces a non-linearity into the sliding motion which can lead to multiple sliding velocities for the same large-scale ice stream geometry, and that switches between these velocities can cause surging behavior. *INDEX TERMS*: 1827 Hydrology: Glaciology (1863); 3210 Mathematical Geophysics: Modeling; 3220 Mathematical Geophysics: Nonlinear dynamics. **Citation**: Schoof, C. (2004), Bed topography and surges in ice streams, *Geophys. Res. Lett.*, 31, L06401, doi:10.1029/2003GL018807.

1. Introduction

[2] Short wavelength bed topography plays an important role in generating drag on glaciers sliding over a hard, undeformable bed [Paterson, 1994, chapter 7]. If the bed is deformable and short-wavelength roughness is easily eroded, drag generation is suppressed. However, assemblies of larger obstacles such as drumlin fields may still provide significant resistance to flow over a weak deformable bed, particularly at high sliding velocities [Schoof, 2002b]. The cores of bed features of this type often show little or no large-scale deformation [e.g., Sharpe, 1987], indicating that they were stationary features rather than being moved by the ice.

[3] Sliding over obstacles whose wavelengths are comparable with ice thickness differs from classical hard-bed sliding [Nye, 1969] because of the presence of the upper, free boundary of the ice. After an initial transient, rapid ice flow over this type of bed topography leads to a steady surface expression in the form of a standing wave [Gudmundsson *et al.*, 1998], whose shape depends not only on the bed obstacles but also on the bulk flow velocity of the ice. In turn, the standing wave affects the stress field at the bed and hence the sliding velocity. In this paper, we demonstrate that the intrinsic non-linearity of this mechanism can lead to more than one surface wave being stable for a given driving stress, corresponding to more than one feasible bulk flow velocity. We also show that the consequent multi-valuedness in the ice flux-driving stress relationship can lead to surging behavior in an ice stream.

[4] Temporally and spatially varying flow velocities in glaciers and ice sheets, and surging behavior in particular,

are well-documented [e.g., Kamb *et al.*, 1985; Retzlaff and Bentley, 1993] and are typically thought to be associated with switches in basal hydrology [Kamb, 1987; Fowler, 1987], thermal feedbacks [van der Veen and Whillans, 1996; Raymond, 2000; Tulaczyk *et al.*, 2000; Hindmarsh and LeMeur, 2001] or changes in the buttressing effect of ice shelves resulting from increased calving [Schmeltz *et al.*, 2002]. The purpose of the present paper is to illustrate a previously unrecognized, purely mechanical phenomenon that causes flow variability.

2. The Model

[5] The model used here [Schoof, 2002a, 2002b] employs a multiple scales expansion [e.g., Holmes, 1995] to separate the ice flow problem into two parts. An ‘inner’ problem in terms of the coordinates (x, z, t) (position and time scaled with ice thickness and the associated convective timescale) quantifies the generation of drag by a local ice flow over bed topography. The evolution of the ice stream as a whole is tracked by an ‘outer’ problem in terms of the coordinates (X, T) (down-stream distance and time scaled with ice stream length and the corresponding convective time scale, respectively). Given a typically small aspect ratio ϵ for the ice stream we have $(X, T) = \epsilon(x, t)$. Importantly, in the asymptotic limit $\epsilon \rightarrow 0$, the two sets of coordinates can be treated as independent.

[6] We assume further that typical bed slopes v are small: the scalings below put $v^2 = \epsilon$. Consequently our model does not deal with large-amplitude bed topography (e.g., mountain ranges), and requires sliding to be fast compared with internal deformation [Schoof, 2002b].

[7] The dimensionless inner problem of finding the local variations $\mathbf{u} = (u, w)$ about a regional mean plug flow velocity U in the x -direction, and the corresponding pressure variations p about a mean field, can be written as [Schoof, 2002a, chapter 4]

$$\nabla^2 \mathbf{u} - \nabla p = \mathbf{0}, \quad \nabla \cdot \mathbf{u} = 0, \quad \text{on } 0 < z < S, \quad (1)$$

$$u_z + w_x = 0, \quad w = Uh_x, \quad \text{on } z = 0, \quad (2)$$

$$u_z + w_x = 0, \quad d = p - 2w_z, \quad w = d_t + Ud_x, \quad \text{on } z = S. \quad (3)$$

Here, $\nabla = (\partial/\partial x, \partial/\partial z)$ and subscripts denote partial derivatives, *viz.* $u_z = \partial u/\partial z$ etc. S is a regionally smoothed ice thickness, while h and d stand for local bed topography and the corresponding surface wave, respectively.

[8] Importantly, S depends only on (X, T) and U depends on (X, t, T) but not on x . The relation determining sliding velocity U enforces horizontal force balance:

$$-SS_X = \langle (p - 2w_z)|_{z=0} h_x \rangle + \tau_b(U), \quad (4)$$

where $\langle \cdot \rangle$ is a spatial average over the inner distance x , and $\tau_b(U)$ is a sliding law describing drag due to flow over small-scale bed roughness [Paterson, 1994, chapter 7]. S evolves as

$$S_T + (\bar{U}S)_X = b(X), \quad (5)$$

where $\bar{U} = \lim_{\tau \rightarrow \infty} \tau^{-1} \int_0^\tau U(X, t, T) dt$ denotes an average over the short timescale, while $b(X)$ is an accumulation rate, assumed given.

[9] The equations above can be motivated without their lengthy formal derivation: Equations (1), (2) and (4) are the Nye-Kamb model for sliding in the absence of regelation [Nye, 1969; Kamb, 1970]. The boundary conditions (3) simply introduce an upper free surface which is stress-free (first and second equalities of (3)) and satisfies a kinematic boundary condition (third equality of (3)). Equation (5) is the usual mass conservation equation for a plug flow. In common with Nye-Kamb sliding theory, the model uses a constant viscosity rather than Glen's law for ice [Paterson, 1994, p. 91]. Our results therefore indicate the possibility of a new mechanism for ice stream variability rather than provide a quantitative proof.

3. A Multi-Valued Geometry-Flux Relationship

[10] The inner problem (1)–(4) provides a relationship between the flux $S\bar{U}$ and the smoothed geometry of the ice stream defined by $S(X, T)$. We consider only the simplest case of a sinusoidal bed $h(x) = \cos(x)$ with no drag generated by small-scale roughness, so $\tau_b \equiv 0$. These assumptions illustrate the essential features of the model.

[11] If we seek solutions for the surface wave of the form $d(x, X, t, T) = \alpha(X, t, T)\cos(x) + \beta(X, t, T)\sin(x)$, the inner problem reduces to

$$\alpha_t = U\beta - F_1(S)\alpha \quad (6a)$$

$$\beta_t = F_2(S)U - U\alpha - F_1(S)\beta \quad (6b)$$

$$\tau_d = G_1(S)U + G_2(S)\beta \quad (6c)$$

where $\tau_d = -SS_X$. The functions F_1 , F_2 , G_1 and G_2 arise from a Fourier transform solution of (1)–(4) [Schoof, 2002a, section 4.5]:

$$F_1(S) = \frac{\sinh^2 S}{2(\sinh S \cosh S + S)},$$

$$F_2(S) = \frac{S \cosh S + \sinh S}{\sinh S \cosh S + S},$$

$$G_1(S) = \frac{\sinh^2 - S^2}{\sinh S \cosh S + S},$$

$$G_2(S) = \frac{S \cosh S + \sinh S}{2(\sinh S \cosh S + S)}.$$

S and hence τ_d , F_1 , F_2 , G_1 and G_2 depend only on the outer coordinates X and T . Consequently, (6) is a set of coupled non-linear ordinary differential equations for α and β with t as the independent variable and τ_d , F_1 , F_2 , G_1 and G_2 acting as parameters that are independent of t . The non-linearity of these equations comes about through the dependence of the sliding velocity U on the surface wave coefficient β

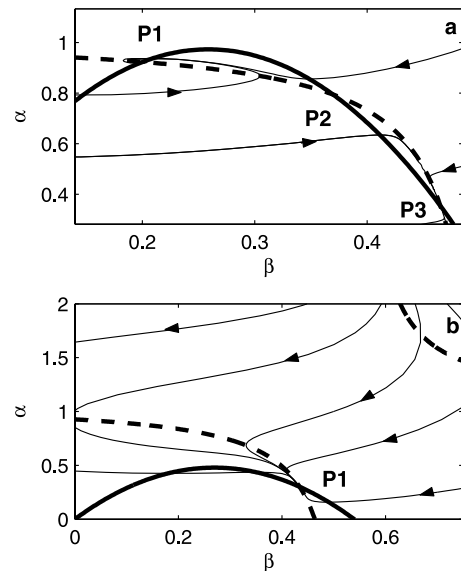


Figure 1. Phase-plane for (6) when $\tau_d = 0.25$, $S = 1$ (panel a) and $\tau_d = 0.25$, $S = 1.25$ (panel b), with the direction of phase-paths indicated by arrows. Nullclines are plotted as heavy solid lines for $\alpha_t = 0$ and as heavy broken lines for $\beta_t = 0$. Intersections of nullclines are critical points, labelled P1–P3. In (a), P1 and P3 are stable while P2 is not. In (b), P1 is stable.

through (6c). This dependence sets our analysis apart from that of Gudmundsson [2003]: In his work, the bulk flow velocity U is prescribed at leading order by a sliding law, and the effect of topography-induced ‘form drag’ appears only at higher order. By contrast, bed and surface topography play a leading-order role in determining U in our model, and cause the non-linearity that is absent in other models.

[12] The large t behaviour of (α, β) determines the final shape of the surface wave and the time-average \bar{U} through (6c). An analysis of the (α, β) phase-plane indicates that the system (6) relaxes to a steady state at large t . Hence a standing wave is formed and U approaches a limit as $t \rightarrow \infty$, whence $\bar{U}(X, T) = \lim_{t \rightarrow \infty} U(X, t, T)$. Schoof [2002a, section 4.5.1] shows that the system (6) can have either one or three critical points (where $\alpha_t = \beta_t = 0$, see Figure 1), corresponding to U given by the real roots of

$$\tau_d = G_1 U + \frac{F_1 F_2 G_2 U}{F_1 + U^2}. \quad (7)$$

In the case of three roots, only the smallest and largest values of U correspond to stable critical points, which will be approached as $t \rightarrow \infty$ for suitable initial values. The third critical point is then unstable, and does not correspond to a steady surface wave which will be formed in practice. By contrast, the critical point corresponding to a single root of (7) is always stable.

[13] For those combinations of S and $-S_X$ for which (7) (into which S and $-S_X$ enter through τ_d , F_1 , F_2 , G_1 and G_2) has three roots, there are two attainable flux states $S\bar{U}$, corresponding to the two stable critical points of (6). Figure 2 shows how the values $S\bar{U}$ corresponding to stable

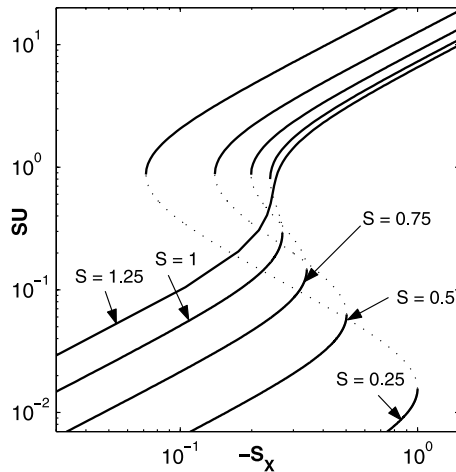


Figure 2. Flux $S\bar{U}$ as a function of negative surface slope $-S_X$ for a number of ice thicknesses S , attainable flux values — corresponding to stable critical points of (6) are plotted as solid lines. Unattainable values — corresponding to unstable critical points — are plotted as dotted lines. Note that Nye-Kamb sliding is retrieved in the large S limit (not shown here).

fixed points of (6) depend on surface slope $-S_X$ for a variety of ice thicknesses S . This figure demonstrates that flux is usually an increasing function of $-S_X$, so (5) is apparently a non-linear diffusion problem, which renders it similar to classical shallow-ice theory [Hutter, 1983]. However, for sufficiently small values of the ice thickness S and the surface slope $-S_X$, the relationship between flux and surface slope is multi-valued. This renders the problem essentially different from ordinary diffusion.

4. Solution of the Ice Stream Problem

[14] Before proceeding with a numerical solution of the outer problem, some minor alterations are required. In order to avoid spatial discontinuities in velocity U , we include longitudinal stresses on the outer length scale. Retention of higher order terms motivates writing $\tau_d = 4\epsilon(SU_X)_X - SS_X$, where the additional term is a depth-integrated mean longitudinal stress. Equation (6) becomes

$$4\epsilon(SU_X)_X - G_1 U = G_2 \beta + SS_X \quad (8a)$$

$$\alpha_t = U\beta - F_1 \alpha \quad (8b)$$

$$\beta_t = F_2 U - \alpha - F_1 \beta. \quad (8c)$$

The original inner problem (6) can be retrieved by ignoring the $O(\epsilon)$ term in (8a). However, this is a singular approximation, which becomes invalid where U changes rapidly with X . Steady states of (8) obey an elliptic equation of the type used to model shelf-like ice streams [MacAyeal, 1989]. Importantly, there can be multiple solutions, not all of which need to be stable.

[15] We assume that there is a symmetric ice divide at $X = 0$, so $U = S_X = 0$ there. In order to avoid the singularity

associated with $S = 0$ at the margin, we assume that there is a calving front at a position $X = X_f(T)$ where S takes a small constant value S_f . Mass conservation then requires

$$\frac{dX_f}{dT} = \frac{S_T}{S_X} \Big|_{X=X_f}$$

This device can be motivated by assuming that the ice stream ends in a shallow lake, where it calves when its thickness is close to floatation [cf. van der Veen, 1996; Vieli *et al.*, 2001]. Importantly, the results obtained are not sensitive to S_f , so long as S_f is small. At $X = X_f$, we apply the usual stress boundary condition for a calving front at flotation [Morland, 1987], $U_X = (1 - r)S_f/(8\epsilon r)$ in dimensionless terms. Here r is the ratio of ice to water density.

[16] Equations (5) and (8) with $\alpha_t = \beta_t = 0$ are first transformed to a fixed spatial domain and then solved by a finite difference scheme with an implicit time step. We assume that switches from fast to slow sliding or vice versa correspond to situations where a stable, steady solution of (8) close to the solution at the previous T -timestep does not exist. One disadvantage of our insistence on using multiple scales in time is that the transition from one flow mode to the other (which presumably occurs on the inner time scale) cannot be resolved. A preferable approach using matched asymptotics will be explored in future work.

[17] Results for one particular choice of parameters are shown in Figure 3. Clearly, the ice surface oscillates

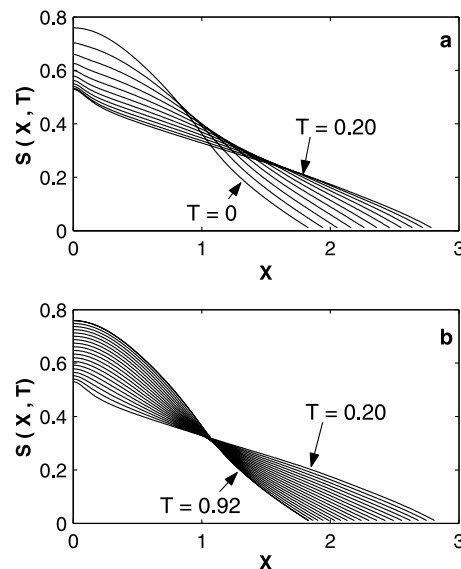


Figure 3. Limit-cycle surge pattern for ice stream with $\epsilon = 0.01$, $b(X) = 1/(1 + X^2) - 1/2$ (which changes from accumulation to ablation at $X = 1$), $r = 0.9$ and $S_f = 0.01$. In panel (a) the surface profile $S(X, T)$ during the surge part of the cycle is shown at T -intervals of 0.02. In panel (b) the slow retreat part of the cycle is shown at T -intervals 0.04. The duration of the surge cycle is 0.92. The sharply concave surface profile which develops near the ice divide in the surge phase occurs because the ice divide has to remain on the slow flux branch, while the remainder of the ice stream is on the fast branch.

between two profiles. The ice stream switches from a slow retreat to a rapid advance when it is short and steep, while the reverse transition occurs when the ice stream is extended and shallow. Numerical experiments further indicate that the profiles at which these switches occur are independent of the initial conditions, a circumstance reminiscent of limit cycle solutions of ordinary differential equations [Coddington and Levinson, 1955]. Multi-valued relationships between surface geometry and flux underpin a number of models of glacier and ice stream surging behavior [Fowler, 1987; Greenberg and Shyong, 1990; Fowler and Schiavi, 1998]. The surge mechanisms in these models are different from ours, but the underlying dynamics are mathematically similar, as they can all be thought of as spatially extended relaxation oscillations.

5. Conclusions

[18] The study of a leading-order model for the flow of an ice stream over an assembly of bed obstacles whose wavelengths are comparable with ice thickness and whose amplitudes are sufficient to cause leading-order drag has indicated that the formation of standing waves at the ice stream surface can lead to multiple flow velocities for the same large-scale ice stream geometry. Each velocity corresponds to a different surface wave configuration. Regular oscillations, or surges, in the ice stream were shown to result from this multi-valuedness in the relationship between ice velocity and surface geometry, which occurs for sufficiently small surface slopes (or sufficiently large bed slopes) and at small ice thicknesses.

[19] A number of open questions still await a satisfactory answer. We have only considered the simplest case of a sinusoidal bed in this paper, whereas actual bed topography is much more complicated. The presence of additional Fourier modes will affect the relationship between flux and geometry derived in section 3, as will the possible formation of cavities. In addition, the effect of a non-linear rheology [Paterson, 1994, chapter 5] on the generation of drag by finite-wavelength bed obstacles remains to be resolved. The process considered in this paper will also interact with other processes usually thought to be responsible for ice stream variability and surging behavior, such as thermal feedbacks in the sliding behavior of the ice stream. For instance, when a change in surface wave configuration leads to a transition from fast to slow flow, heat generation at the bed will be reduced and flow velocities will be reduced further, possibly leading to a complete shutdown of the ice stream. Basal melting due to ice thickening will have to recommence before a new surge cycle can be started.

[20] **Acknowledgments.** Financial support from a Killam postdoctoral research fellowship at UBC is gratefully acknowledged.

References

- Coddington, E. A., and N. Levinson (1955), *Theory of Ordinary Differential Equations*, McGraw-Hill, New York.
- Fowler, A. C. (1987), A theory of glacier surges, *J. Geophys. Res.*, *92*(B9), 9111–9120.
- Fowler, A. C., and E. Schiavi (1998), A theory of ice-sheet surges, *J. Glaciol.*, *44*(146), 104–118.
- Greenberg, J. M., and W. Shyong (1990), Surging glacial flows, *IMA J. Appl. Math.*, *45*(3), 195–223.
- Gudmundsson, G. H. (2003), Transmission of basal variability to a glacier surface, *J. Geophys. Res.*, *108*(B5), 2253, doi:10.1029/2002JB002107.
- Gudmundsson, G. H., C. F. Raymond, and R. Bindshadler (1998), The origin and longevity of flow stripes on Antarctic ice streams, *Ann. Glaciol.*, *27*, 145–152.
- Hindmarsh, R. C. A., and E. LeMeur (2001), Dynamical processes involved in the retreat of marine ice sheets, *J. Glaciol.*, *47*(157), 271–282.
- Holmes, M. H. (1995), *Introduction to Perturbation Methods*, Springer-Verlag, New York.
- Hutter, K. (1983), *Theoretical Glaciology*, D. Reidel, Norwell, Mass.
- Kamb, B. (1970), Sliding motion of glaciers: Theory and observation, *Rev. Geophys.*, *8*(4), 673–728.
- Kamb, B. (1987), Glacier surge mechanism based on linked cavity configuration of the basal water conduit system, *J. Geophys. Res.*, *92*(B9), 9083–9100.
- Kamb, B., C. F. Raymond, W. D. Harrison, H. Engelhardt, K. A. Echelmeyer, N. Humphrey, M. M. Brugman, and T. Pfeffer (1985), Glacier surge mechanism: 1982–1983 surge of Variegated Glacier, Alaska, *Science*, *227*(4686), 469–479.
- MacAyeal, D. R. (1989), Large-scale flow over a viscous basal sediment: Theory and application to Ice Stream E, Antarctica, *J. Geophys. Res.*, *94*(B4), 4017–4087.
- Morland, L. W. (1987), Unconfined ice-shelf flow, in *Dynamics of the West Antarctic Ice Sheet*, edited by C. J. van der Veen and J. Oerlemans, pp. 99–116, D. Reidel, Norwell, Mass.
- Nye, J. F. (1969), A calculation of the sliding of ice over a wavy surface using a Newtonian viscous approximation, *Proc. R. Soc. London, Ser. A*, *311*, 445–467.
- Paterson, W. S. B. (1994), *The Physics of Glaciers*, 3rd ed., Pergamon, New York.
- Raymond, C. F. (2000), Energy balance of ice streams, *J. Glaciol.*, *46*(155), 665–674.
- Retzlaff, R., and C. R. Bentley (1993), Timing of stagnation of Ice Stream C, West Antarctica, from short-pulse radar studies of buried crevasses, *J. Glaciol.*, *39*(133), 553–561.
- Schmeltz, M., E. Rignot, T. K. Dupont, and D. R. MacAyeal (2002), Sensitivity of Pine Island Glacier, West Antarctica, to changes in ice-shelf and basal conditions: A model study, *J. Glaciol.*, *48*(163), 552–558.
- Schoof, C. (2002a), Mathematical models of glacier sliding and drumlin formation, DPhil thesis, Univ. of Oxford, Oxford, UK.
- Schoof, C. (2002b), Basal perturbations under ice streams: Form drag and surface expression, *J. Glaciol.*, *48*(162), 407–416.
- Sharpe, D. S. (1987), The stratified nature of drumlins from Victoria Island and southern Ontario, Canada, in *Drumlin Symposium*, edited by J. Menzies and J. Rose, pp. 185–214, A. A. Balkema, Brookfield, Vt.
- Tulaczyk, S., W. B. Kamb, and H. F. Engelhardt (2000), Basal mechanisms of Ice Stream B, West Antarctica: 2. Undrained plastic bed model, *J. Geophys. Res.*, *105*(B1), 483–494.
- van der Veen, C. J. (1996), Tidewater calving, *J. Glaciol.*, *42*(141), 375–385.
- van der Veen, C. J., and I. M. Whillans (1996), Model experiments on the evolution and stability of ice streams, *Ann. Glaciol.*, *23*, 129–137.
- Vieli, A., M. Funk, and H. Blatter (2001), Flow dynamics of tidewater glaciers: Numerical modelling approach, *J. Glaciol.*, *47*(159), 595–606.

C. Schoof, Department of Earth and Ocean Sciences, University of British Columbia, 6339 Stores Road, Vancouver, British Columbia, Canada, V6T 1Z4. (cschoof@eos.ubc.ca)